

Pairwise Check Decoding for LDPC Coded Two-Way Relay Block Fading Channels

Jianquan Liu, Meixia Tao and Youyun Xu

Abstract

Partial decoding is known to have the potential to achieve a larger rate region than that of full decoding in two-way relay (TWR) channels. Existing partial decoding realizations are however designed for Gaussian channels and with a static physical layer network coding (PLNC) mapping. In this paper, we propose a new channel coding solution at the relay, called *pairwise check decoding* (PCD), for low-density parity-check (LDPC) coded TWR system over block fading channels. The main idea is to form a check relationship table (check-relation-tab) for the superimposed LDPC coded packet pair in the multiple access (MA) phase in conjunction with an adaptive PLNC mapping in the broadcast (BC) phase. Using PCD, we then present a partial decoding method, two-stage closest-neighbor clustering with PCD (TS-CNC-PCD), with the aim of minimizing the worst pairwise error performance. Moreover, a kind of correlative rows optimization, named as the minimum correlation optimization (MCO), is proposed for selecting the better check-relation-tabs. Simulation results confirm that the proposed TS-CNC-PCD has wonderful convergence behaviors and significant coding gains for certain TWR Gaussian channels. For TWR fading channels, the TS-CNC-PCD also outperforms the conventional XOR with belief propagation (BP) obviously.

Index Terms

Two-way relaying, block fading channel, LDPC, physical layer network coding, partial decoding, pairwise check decoding, closest-neighbor clustering.

This work was partly presented in IEEE ICC 2010 [1] and IEEE ICC 2011 [2].

Jianquan Liu, Meixia Tao and Youyun Xu are with the Department of Electronic Engineering, Shanghai Jiao Tong University, Shanghai, 200240, P. R. China (e-mails: {jianquanliu, mxtao, xuyouyun}@sjtu.edu.cn).

I. INTRODUCTION

Two-way relaying, where two source nodes exchange information with the help of a relay node, has recently gained a lot of research interests [3]–[9]. It is shown able to overcome the half-duplex constraint and significantly improve the system spectral efficiency in relay-based cooperative networks. Upon receiving the bidirectional information flows, the relay node combines them together and then broadcasts to the two desired destinations. The operation at the relay resembles network coding [10], a technique originally developed for wireline networks. It is thus often referred to as physical layer network coding (PLNC) [7] or analog network coding (ANC) [8].

Among the various two-way relaying strategies, the two practical and efficient ones are known as amplify-and-forward (AF) and decode-and-forward (DF), similar to those in one-way relaying. Different from one-way relaying, the DF strategy for two-way relaying further includes full DF [11], [12] and partial DF [13]–[15]. This is because the combining process operated at the relay is a many-to-one mapping (e.g. $1 \oplus 1 = 0 \oplus 0 = 0$). As a result, it is not necessary for the relay to fully decode the message pair before combining them together. Being a simple realization of partial DF, the denoise-and-forward (DNF) strategy proposed in [16] demonstrates significant performance gain over the full DF. It is also known that partial decoding has the potential to achieve a much larger rate region than full decoding, even though its capacity region is still unknown. Consequently, it remains as a fundamental and challenging task to realize the potential of partial decoding in two-way relay (TWR) channels through practical coding and modulation techniques.

Several works have been reported on the implementations of partial DF for channel-coded TWR systems, and they are also known as joint network-coding and channel-coding (JNCD) design in the literature. An intuitive method is to utilize the fact that the network-coded (eg. XOR or modulo addition) codeword pair is also a valid codeword given the same linear code (e.g. LDPC or Lattice codes) applied at both source codes [17]–[20]. In this method, the relay first computes the probability of $x_A \oplus x_B$ based on the received superimposed signal y_C during the multiple-access (MA) phase, where x_A and x_B are the symbols after channel coding and modulation from source A and source B , respectively, and then apply soft-decoding to decode the associated network-coded information symbol pair $s_A \oplus s_B$. We refer to this method as partial DF based on conventional XOR. However, this method discards useful information related to the

decoding of the whole packet $s_A \oplus s_B$ during the mapping from signal y_C to the probability of $x_A \oplus x_B$. A more advanced partial decoding method is to exploit the Euclidean distance profile of the superimposed symbol pair after going through the noisy channel in the MA phase [21]. The relay first decodes the arithmetic-sum of the coded symbol pair $c_A + c_B$ and then map it to $s_A \oplus s_B$ for broadcasting. The authors in [21] show that this partial DF method based on arithmetic-sum provides higher decoding gain than the one based on conventional XOR. Note that both aforementioned methods are designed specifically for symmetric and Gaussian channels.

For TWR channel with fading, the conventional XOR does not always work well due to the undesired phase and amplitude offset between the two TWR channels in the MA phase. Authors in [22] therefore proposed an adaptive network coding with respect to the instantaneous channel fading, named as closest-neighbor cluster (CNC) mapping. Compared to the conventional XOR, the CNC mapping obtains a higher end-to-end throughput. To further ensure reliable communication, the authors extended this method for convolutional-coded system in [23] and discussed the code design based on trellis-coded modulation (TCM) [24, Section 8.2]. However, this TCM-based CNC mapping requires to change the coding structure at the two source nodes and switches two transmission protocols (CNC DNF and pseudo AF) in order to exploit the system performance.

In this paper, we propose a new relay channel coding solution, called *pairwise check decoding* (PCD), for LDPC coded TWR fading channels. The main idea is to form a check relationship table (check-relation-tab) for the coded symbol pair (c_A, c_B) by taking both the employed LDPC codes and the adaptive PLNC mapping into accounts. The proposed PCD algorithm is universal for any adaptive PLNC mapping under the constraint of exclusive law. Generally, the proposed PCD approach is a practical and efficient realization of the promising DNF TWR strategy with advanced channel coding. In terms of optimizing the minimum Euclidean distance (MED) between any two codewords, we present a partial decoding method, two-stage CNC with PCD (TS-CNC-PCD), for TWR fading channels. Moreover, a kind of correlative rows optimization, named as the minimum correlation optimization (MCO), is proposed for selecting the better check-relation-tab. Simulation results confirm that the proposed TS-CNC-PCD has wonderful convergence behaviors along with the maximum iteration increasing and significant coding gains compared to the uncoded system for certain TWR Gaussian channels. For TWR fading

channels, the TS-CNC-PCD also outperforms the conventional XOR with belief propagation (BP) obviously.

The rest of the paper is organized as follows. In section II, we present the channel coding model for TWR block fading channels. Section III analyzes the lower bound of the outage probability. The design criterion of partial decoding is interpreted in Section IV. In Section V, we propose the PCD algorithm in details. Section VI present a new partial decoding method, TS-CNC-PCD, based on the proposed PCD approach in terms of optimizing the MED. The convergence behaviors and the coding gains of the proposed PCD algorithm are simulated in Section VII. Finally, we conclude the paper in section VIII.

II. CHANNEL CODING MODEL FOR TWO-WAY RELAY FADING CHANNELS

We consider a TWR fading channel where two source nodes, denoted as A and B , exchange information with the help of a relay node, denoted as C . We assume that all the nodes operate in the half-duplex mode. The channel on each communication link is assumed to be corrupted with block fading and additive white Gaussian noise (AWGN). For simplicity, we also assume the channel gains are reciprocal and unchanged during a whole packet transmission.

The proposed channel coding model is shown in Fig. 1, where the communication takes place in two phases. First, the information packet from each source, denoted as \mathbf{S}_i , for $i \in \{A, B\}$, is encoded individually by a traditional LDPC code with parity check matrix \mathbf{H}_i . Unlike the existing work, we do not impose the constraint that \mathbf{H}_A and \mathbf{H}_B must be identical. Instead, we only require that they have the same size and the same location of non-zero elements. We further assume that the encoder is operated in $\mathbf{GF}(q)$, where $q \in \{2^1, 2^2, 2^3, \dots\}$. Note that q -ary ($q > 2$) coding can improve the performance compared with binary coding. More details can be found in [25]–[27] and references therein. The encoded packet, \mathbf{C}_i , is modulated by using q -ary modulation, such as q -PSK or q -QAM, generating \mathbf{X}_i , and then transmitted simultaneously to the relay node. The n -th symbol of each packet is denoted as $\mathbf{C}_i(n) \in \mathcal{Z}_q$, $\mathcal{Z}_q = \{0, 1, \dots, q-1\}$, and $\mathbf{X}_i(n) \in \mathcal{Q}_q$, respectively. The superimposed packet received by the relay, denoted as \mathbf{Y}_C is given by

$$\mathbf{Y}_C = H_{AC}\mathbf{X}_A + H_{BC}\mathbf{X}_B + \mathbf{W}_C, \quad (1)$$

where $H_{ii'}$ denotes the complex-valued channel coefficient of link from node i to node i' , and $\mathbf{W}_{i'}$ denotes complex AWGN with variance $\sigma_{i'}^2$ of node i' . Therein, $\{i, i'\} \in \{A, B, C\}$.

We assume perfect symbol synchronization at the two sources and perfect channel estimation at the relay. After receiving the superimposed packet, the relay first computes the probability of the adaptive PLNC mapped and coded symbol pair, denoted as $\mathbf{C}_C = \mathcal{M}(\mathbf{C}_A, \mathbf{C}_B)$, based on the instantaneous channel states during the MA phase, then obtains their hard-decision using the proposed PCD, the details of which will be presented in Section V. Here, \mathcal{M} denotes a kind of adaptive PLNC mapping, see for example the CNC mapping in [22]. Note that no full decoding of \mathbf{C}_A and \mathbf{C}_B is needed as an intermediate step. No extra channel encoding at the relay is needed either. Then, the relay broadcasts the modulated coded symbols of \mathbf{C}_C , denoted as \mathbf{X}_C , and mapping rule $\mathcal{M}()$ to two source nodes. The received signals at the nodes A and B are respectively written as

$$\begin{aligned} \mathbf{Y}_A &= H_{CA}\mathbf{X}_C + \mathbf{W}_A; \\ \mathbf{Y}_B &= H_{CB}\mathbf{X}_C + \mathbf{W}_B. \end{aligned} \quad (2)$$

Each source node computes the probability of the desired information $\mathbf{C}_A(\mathbf{C}_B)$ from the received symbols $\mathbf{Y}_B(\mathbf{Y}_A)$ by using the adaptive PLNC mapping rule with the help of its self-information $\mathbf{C}_B(\mathbf{C}_A)$. Lastly, the traditional LDPC decoding algorithm, e.g. BP, is applied, the output of which is the desired information packet $\mathbf{S}_A(\mathbf{S}_B)$. Note that each source node should know the check matrix of the other source.

III. ANALYSIS OF OUTAGE PROBABILITY

In this section, we derive the system outage probability of TWR fading channel, which serves as a good approximation of the achievable frame error rate (FER) in the limit of infinite block length [28]. Here, the system is said to be in outage if the achievable sum-rate falls below a target. Since the capacity region of two-way relaying with partial decoding is still unknown [13]–[15], we resort to the capacity outer bound as follows [12, Theorem 2], based on which a lower bound of the outage probability can be obtained.

$$(R_{AB}, R_{BA}) : \left\{ R_{AB} \leq \min(\beta C_{AC}, (1 - \beta)C_{CB}), R_{BA} \leq \min(\beta C_{BC}, (1 - \beta)C_{CA}) \right\}, \quad (3)$$

where β is the time sharing parameter, R_{ij} and C_{ij} denote the instantaneous data rate and channel capacity of the link from node i to node j , for $i, j \in \{A, B, C\}$, respectively.

After simple manipulation of the constraints in (3), we obtain the following linear inequalities about R_{AB} and R_{BA}

$$\begin{aligned}\frac{R_{AB}}{C_{AC}} + \frac{R_{BA}}{C_{CB}} &\leq 1, \\ \frac{R_{AB}}{C_{AC}} + \frac{R_{BA}}{C_{CA}} &\leq 1, \\ \frac{R_{AB}}{C_{CB}} + \frac{R_{BA}}{C_{BC}} &\leq 1, \\ \frac{R_{BC}}{C_{BC}} + \frac{R_{BC}}{C_{CA}} &\leq 1.\end{aligned}\tag{4}$$

Let us further assume that the TWR channels considered here are reciprocal, i.e. $C_{ij} = C_{ji}$ for $i, j \in \{A, B, C\}$. From (4), we can easily obtain the upper bound of the maximum sum-rate for the considered TWR channels

$$S_u = \max_{(R_{AB}, R_{BA}) \in (3)} R_{AB} + R_{BA} = \min(C_{AC}, C_{BC}),\tag{5}$$

which is also given in [16]. Therein, each of the terms C_{ij} , $i, j \in \{A, B, C\}$, is the channel capacity of a traditional point-to-point channel with input alphabet $x_{ij} \in \mathcal{Q}_q$ and received signal $y_{ij} = \alpha_{ij}x_{ij} + w_{ij}$, where $w_{ij} \sim \mathcal{N}(0, \sigma^2)$ and α_{ij} denotes a real- or complex-valued channel coefficient of the link from node i to j with $\mathbb{E}\{|\alpha_{ij}^2|\} = 1$. The average SNR at node A or B is defined as [29]

$$SNR = \frac{\mathbb{E}\{|\alpha_{ij}^2|\}}{\mathbb{E}\{|w_{ij}^2|\}} = \begin{cases} \frac{1}{\sigma^2}, & \text{one-dimensional modulation,} \\ \frac{1}{2\sigma^2}, & \text{two-dimensional modulation.} \end{cases}$$

With the further assumption of equiprobable channel inputs, extending the well-known formula for the capacity of continuous-valued Gaussian channels [29, Eqs. 3-5] to the case of block fading channels yields

$$C_{ij}(\alpha_{ij}) = \log_2(q) - \frac{1}{q} \sum_{m=0}^{q-1} \mathbb{E} \left\{ \log_2 \sum_{n=0}^{q-1} \exp \left[- \frac{|y_{ij} - \alpha_{ij}x_{ij}^n|^2 - |y_{ij} - \alpha_{ij}x_{ij}^m|^2}{2\sigma^2} \right] \right\}\tag{6}$$

in bit/channel use. Here, \mathbb{E} represents expectation over y_{ij} given $x_{ij} = x_{ij}^m$ and α_{ij} , with x_{ij}^m being an element of the modulated signal sets $\{\mathcal{Q}_q : x_{ij}^0, x_{ij}^1, \dots, x_{ij}^{q-1}\}$.

In addition, we denote the data rate r_{ij} as the average spectral efficiency of the link from node i to node j , $\{i, j\} \in \{A, B\}$, and the target rate of overall system as $S_r = r_{AB} + r_{BA}$. In our considered channel coded TWR model, we have

$$S_r = \beta \left(R_{AB} \log_2^{qAB} + R_{BA} \log_2^{qBA} \right) = \frac{1}{2} \left(R \log_2^q + R \log_2^q \right) = R \log_2^q,\tag{7}$$

where R denotes the channel code rate. Then the outage probability can be lower bounded as

$$P_{out} \geq P(S_u < S_r) = P\left(\min\left\{C_{AC}(\alpha_{AC}), C_{BC}(\alpha_{BC})\right\} < S_r\right), \quad (8)$$

which can be easily evaluated by Monte Carlo averaging over the block fading coefficients and the AWGN.

IV. DESIGN CRITERION OF $\mathcal{M}(\mathbf{C}_A, \mathbf{C}_B)$

Similar to the uncoded system in [22], a necessary condition for successful decoding at two sources/destinations in coded TWR system is for the adaptive PLNC mapping to satisfy the exclusive law:

$$\begin{aligned} \mathcal{M}(\mathbf{C}_A, \mathbf{C}_B) &\neq \mathcal{M}(\mathbf{C}'_A, \mathbf{C}_B), \text{ for all } \{\mathbf{C}_A \neq \mathbf{C}'_A, \mathbf{C}_B\} \in \mathcal{Z}_q, \\ \mathcal{M}(\mathbf{C}_A, \mathbf{C}_B) &\neq \mathcal{M}(\mathbf{C}_A, \mathbf{C}'_B), \text{ for all } \{\mathbf{C}_A, \mathbf{C}_B \neq \mathbf{C}'_B\} \in \mathcal{Z}_q. \end{aligned} \quad (9)$$

Given the above necessary condition, we next discuss the design criterion of $\mathcal{M}(\mathbf{C}_A, \mathbf{C}_B)$ to optimize the system error performance. We aim at minimizing the pairwise error probability (PEP) between two distinct codewords \mathbf{C}'_C and \mathbf{C}''_C in the MA phase because the MA interference dominates the whole system performance. Note that the PEP between different codewords is considered in this work whereas [22] was concerned with the PEP between different uncoded symbols. For TWR fading channels, the PEP between \mathbf{C}'_C and \mathbf{C}''_C conditioned on the $\{H_{AC}, H_{BC}\}$ is given by [30, p. 265] [24, Section 5.5] [31, Eq. 7] [22, Eqs. 5-6]

$$\begin{aligned} P_e(\mathbf{C}'_C \rightarrow \mathbf{C}''_C \mid \{H_{AC}, H_{BC}\}) &= P_e\left(\mathcal{M}(\mathbf{C}'_A, \mathbf{C}'_B) \rightarrow \mathcal{M}(\mathbf{C}''_A, \mathbf{C}''_B) \mid \{H_{AC}, H_{BC}\}\right) \\ &= Q\left(\sqrt{\frac{\zeta_C D_{ll'}^2 \{H_{AC}, H_{BC}\}}{2\sigma^2}}\right), \end{aligned} \quad (10)$$

where ζ_C and σ^2 are the energy per coded symbol and the variance of Gaussian noise at relay node C, respectively, and $D_{ll'}^2$ represents the squared Euclidean distance between the codewords \mathbf{C}'_C and \mathbf{C}''_C and is the function of two channel coefficients $\{H_{AC}, H_{BC}\}$ given by

$$D_{ll'}^2 = \sum_{i=1}^n \left[\hat{x}_l(i) - \hat{x}_{l'}(i)\right]^2. \quad (11)$$

In (11), n denotes the length of transmitted codewords and

$$\begin{aligned} \hat{x}_l(i) &= H_{AC}x'_A(i) + H_{BC}x'_B(i), \\ \hat{x}_{l'}(i) &= H_{AC}x''_A(i) + H_{BC}x''_B(i). \end{aligned} \quad (12)$$

From (10), it is clear that to minimize the pairwise error probability, one should design a mapping rule $\mathbf{C}_C = \mathcal{M}(\mathbf{C}_A, \mathbf{C}_B)$ that can maximize the MED between any pair of codewords $(\mathbf{C}_C^l, \mathbf{C}_C^{l'})$. We denote it as

$$E^2 = \min_{\mathcal{M}(\mathbf{C}_A^l, \mathbf{C}_B^l) \neq \mathcal{M}(\mathbf{C}_A^{l'}, \mathbf{C}_B^{l'})} D_{ll'}^2. \quad (13)$$

V. PROPOSED PAIRWISE CHECK DECODING (PCD)

Since the existing two solutions, namely, conventional XOR [17], [18] and arithmetic-sum [21] can not arbitrarily map the neighboring symbol pairs to one symbol only subject to the exclusive law (9), it then remains to find a channel coding solution that can maximize the MED according to (10) and (13).

We consider a representative received signal constellation at the relay node shown in Fig. 2(c), where $H_{BC} \approx H_{AC}e^{j\pi/4}$. Therein, two source nodes use the traditional GF(4) LDPC encoder and QPSK modulation. For the conventional XOR mapping, we have $\mathbf{C}_C = \mathbf{C}_A \oplus \mathbf{C}_B$ while for the arithmetic-sum solution we have $\mathbf{C}_C = \mathbf{C}_A + \mathbf{C}_B$. Based on the CNC mapping principle [22], the symbol pairs $\{(0, 1), (1, 2)\}$, $\{(2, 0), (0, 3)\}$, $\{(2, 1), (3, 2)\}$ or $\{(3, 0), (1, 3)\}$ should be mapped together in order to maximize the symbol distance between two PLNC mapped symbols, as depicted in Fig. 2(c). However, $0 \oplus 1 \neq 1 \oplus 2$, $2 \oplus 0 \neq 0 \oplus 3$, $2 \oplus 1 \neq 3 \oplus 2$, $3 \oplus 0 \neq 1 \oplus 3$ (using conventional XOR) and $0 + 1 \neq 1 + 2$, $2 + 0 \neq 0 + 3$, $2 + 1 \neq 3 + 2$, $3 + 0 \neq 1 + 3$ (using arithmetic-sum). Note that maximizing the symbol-wise Euclidean distance does not always lead to error probability minimization in coded systems, we here just state the necessity of proposing a new channel coding solution for applying the special PLNC mapping. In the rest of this section, we will propose the PCD approach, which can solve aforementioned puzzle.

A. Check relationship table (check-relation-tab) at relay

At first, we set forth some notations. We assume that two LDPC codes \mathbf{H}_A and \mathbf{H}_B are used at the two sources. The two parity check matrices have the same size of $M \times N$ and the same locations of non-zero's. Let h_{mn}^A and h_{mn}^B denote the elements at the m -th row and n -th column of \mathbf{H}_A and \mathbf{H}_B , respectively. $M_m = \{n : h_{mn} \neq 0\}$ denote the set of column locations of the non-zero's in the m -th row; $M_{m \setminus n} = \{n' : h_{mn'} \neq 0\} \setminus \{n\}$ denotes the set of column locations of the non-zero's in the m -th row, excluding location n ; $N_n = \{m : h_{mn} \neq 0\}$ denotes the set of row locations of the non-zero's in the n -th column; $N_{n \setminus m} = \{m' : h_{m'n} \neq 0\} \setminus \{m\}$ denotes

the set of row locations of the non-zero's in the n -th column, excluding location m . Note that in the following sections the arithmetic operations are all in $\mathbf{GF}(q)$ unless specified otherwise.

It is clear that, the traditional BP decoding algorithm [32], [33] can be applied effectively once the check matrix of a LDPC code is given under conventional XOR pattern. However, if the adaptive PLNC mapping is applied, given alone the individual check matrices of the LDPC codes applied at both source nodes, the packet pairs cannot be decoded directly. Instead, the constraint relationship regarding symbol pairs in the two packets should be derived. In this subsection, we introduce a so-called check-relation-tab to describe such symbol pair constraints.

1) *Check-relation-tab*: Considering the encoding characteristics of \mathbf{H}_A and \mathbf{H}_B , we have the constraint equations for each m row as follows:

$$\begin{aligned} \sum_{n \in M_m} \mathbf{C}_A(n) \times h_{mn}^A &= 0, \\ \sum_{n \in M_m} \mathbf{C}_B(n) \times h_{mn}^B &= 0. \end{aligned} \tag{14}$$

Note that we should obtain M check-relation-tabs for M pairs of correlative rows, which belong to two LDPC codes respectively. The m -th check-relation-tab (also referred to as the joint constraint of the symbol pairs $\{\mathbf{C}_A(n), \mathbf{C}_B(n)\}$ at locations $n \in M_m$) is only constrained by the row weight and non-zero elements of two correlative m -th rows. It consists of two parts, one for virtual encoder, and the other for PCD decoder. In virtual encoder, without loss of generality, we assume that the symbol pair $\{\mathbf{C}_A(n), \mathbf{C}_B(n) \in \mathcal{Z}_q\}$ at a random location n is not known. Thus, we obtain the possible values for $\{\mathbf{C}_A(n), \mathbf{C}_B(n)\}$ at the given n base on (14) through enumerating all values for $\{\mathbf{C}_A(n), \mathbf{C}_B(n)\}$ at locations $n \in M_{m \setminus n}$. Then, the symbol pairs $\{\mathbf{C}_A(n), \mathbf{C}_B(n)\}$ at all locations $n \in M_m$ are mapped to $\mathbf{C}_C(n) \in \mathcal{Z}_{q'}, q \leq q' \leq q^2$.

Since the number of symbol pairs $\{\mathbf{C}_A(n), \mathbf{C}_B(n)\}$ mapped to each element $\mathbf{C}_C(n)$ may not be the same, the probability of occurrence for each element $\mathbf{C}_C(n)$ should be computed separately. Without loss of generality, we assume that the element $\mathbf{C}_C(n)$ at location n is known. That is to say, which one of the symbol pairs mapped to $\mathbf{C}_C(n)$ is assured. Then, we should compute the probability of occurrence for the corresponding possible values $\mathbf{C}_C(n)$ at locations $n \in M_{m \setminus n}$ by classifying the aforementioned probability of each element which is generated by the virtual encoder.

As an example, we present the panoramic Tanner Graph of a virtual LDPC code at the relay with \mathbf{H}_A and \mathbf{H}_B in Fig. 3(a), where the code length is 12 and the row weight and column

weight are 6 and 3 respectively as shown below.

$$\mathbf{H}_A = \mathbf{H}_B = \begin{bmatrix} 1 & 0 & 1 & 0 & 1 & 0 & 1 & 0 & 1 & 0 & 0 & 1 \\ 0 & 1 & 0 & 1 & 0 & 1 & 0 & 1 & 0 & 1 & 1 & 0 \\ 1 & 1 & 1 & 1 & 1 & 1 & 0 & 0 & 0 & 0 & 0 & 0 \\ 0 & 0 & 0 & 0 & 0 & 0 & 1 & 1 & 1 & 1 & 1 & 1 \\ 1 & 1 & 1 & 0 & 0 & 0 & 1 & 1 & 1 & 0 & 0 & 0 \\ 0 & 0 & 0 & 1 & 1 & 1 & 0 & 0 & 0 & 1 & 1 & 1 \end{bmatrix}$$

The solid circles and squares denote the check functions at each source node, while non-solid circles and squares denote the transmitted symbols of a code. In like manner, the solid and non-solid ellipses denote the check functions and the corresponding received symbol pairs. f_r^s denote the r -th check functions of the LDPC code at node s , where $r \in [0, 5]$, $s \in \{A, B, C\}$.

Next, we will derive the check function of f_0^C from f_0^A and f_0^B using the segmental Tanner graph in Fig. 3(b), which is separated from the Fig. 3(a). l_n denotes the symbol pair $(\mathbf{C}_A(n), \mathbf{C}_B(n))$, for $n \in [0, 11]$. The principle of the PLNC mapping between l_n and $\{a, b, c, d\}$ is determined only by the exclusive law (9). Let $\{\eta_n \in \mathcal{Z}_q\}$ and $\{\xi_n \in \mathcal{Z}_q\}$ denote the non-zero elements of the 0-th row of \mathbf{H}_A and \mathbf{H}_B , we have the constraint equations as follows:

$$\begin{aligned} \sum_{n \in \{0, 2, 4, 6, 8, 11\}} \mathbf{C}_A(n) \times \eta_n &= 0, \\ \sum_{n \in \{0, 2, 4, 6, 8, 11\}} \mathbf{C}_B(n) \times \xi_n &= 0, \end{aligned} \quad (15)$$

We consider all 4 possible clustering methods of the symbol pairs, as shown in Tab. I, in order to indicate that our proposed PCD approach can deal with any PLNC mapping under the exclusive law (9). Each symbol pair $(\mathbf{C}_A(n), \mathbf{C}_B(n))$ is mapped to one of the four $\{a, b, c, d\}$, three $\{a, b, c\}$ or two $\{a, b\}$ elements. Here, to avoid confusion, we let $\{a, b, c, d\}$, $\{a, b, c\}$ and $\{a, b\}$ indicate the decoding symbols (not broadcasted symbols) during the period of operating PCD algorithm.

For the especial \mathcal{M}_0 mapping, there is no clustering operated between any two symbol pairs. However, the pairwise check function $f_0^C \neq f_0^A = f_0^B$ because the features of linear block codes are not valid here. Without loss of generality, we assume that the symbol pairs l_0, l_2, l_4, l_6 and l_8 have been known, e.g. $l_0 = a, l_2 = c, l_4 = d, l_6 = a$ and $l_8 = b$, as shown in (1) of the Fig. 3(b). The possible value for the symbol pair l_{11} can be obtained by (15). It is important to note that each element constrained by the pairwise check functions f_n^C corresponds to one

symbol pair in $\{l_n, n \in \{0, 2, 4, 6, 8, 11\}\}$, the range of which is in $\{a, b, c, d\}$. Note that we should operate $P(0) = P(a) + P(d)$, $P(1) = P(b) + P(c)$ before hard decision. Therein, $P(i)$ denotes the probability of occurrence of the element i , and $\{0, 1\}$ indicate the PLNC mapped symbols which will be transmitted in BC phase.

Considering the \mathcal{M}_1 (\mathcal{M}_2) mappings, the symbol pairs $(0, 1)$ and $(1, 0)$ ($(0, 0)$ and $(1, 1)$) should be clustered to the same symbol $\{b\}$ ($\{a\}$). That is to say, $\{b\}$ ($\{a\}$) in \mathcal{M}_1 (\mathcal{M}_2) has two possible values while $\{b\}$ ($\{a\}$) in \mathcal{M}_0 only has one value $(0, 1)$ ($(0, 0)$). At the same time, the range of $\{l_n, n \in \{0, 2, 4, 6, 8, 11\}\}$ is in $\{a, b, c\}$ for both the \mathcal{M}_1 and \mathcal{M}_2 mappings, as shown in (2) of the Fig. 3(b). Different from \mathcal{M}_0 mapping, $P(0) = P(a) + P(c)$ and $P(1) = P(b)$ ($P(0) = P(a)$ and $P(1) = P(b) + P(c)$) should be carried out for \mathcal{M}_1 (\mathcal{M}_2) mapping before the hard decision. Lastly, we cluster two symbol pairs $(0, 0)$ and $(1, 1)$ to $\{a\}$ and the remainder to $\{b\}$ in the \mathcal{M}_3 mapping. Here both $\{a\}$ and $\{b\}$ have two possible values and the range of $\{l_n, n \in \{0, 2, 4, 6, 8, 11\}\}$ is in $\{a, b\}$ consequently, as shown in (3) of the Fig. 3(b).

Now, the so-called check-relation-tabs for 4 PLNC mappings in the Tab. I are generated, as shown in Tables II and III. Here, F_W is the weighted factor which should be multiplied with the probability of the five elements behind. Then, we just need to compute the probability of occurrence of the corresponding possible values $\{a, b, c, d\}$ for l_0, l_2, l_4, l_6 and l_8 one by one. However, using the binary LDPC codes or the q -ary ($q > 2$) codes with the non-zero elements $\{\eta, \dots, \eta \in \mathcal{Z}_q\}$, we have the same probability distribution of occurrence among $\{l_n, n \in \{0, 2, 4, 6, 8, 11\}\}$ for each PLNC mapping, like $f_r^s = f_{r'}^s, r \neq r'$.

B. Pairwise check decoding (PCD) algorithm

After obtaining the check-relation-tab, the PCD algorithm can be readily carried out. Note that the locations of non-zeros in the q -ary LDPC codes used at two source nodes are still valid here. We only change the check functions of symbol pairs from $\{f_r^A, f_r^B\}$ to f_r^C by the derived check-relation-tab. Let $u_n^k = Pr(\mathbf{C}_C(n) = k | \mathbf{Y}(n))$; $v_m^k = Pr(f_m^C \text{ satisfied} | \mathbf{C}_C(n) = k, \mathbf{Y}(n))$; $t_{nm} = (u_n^k, k \in \mathcal{Z}_{q'})$, $q \leq q' \leq q^2$, denotes the messages to be passed from symbol node $\mathbf{C}_C(n)$ to check node f_m^C ; $w_{mn} = (v_m^k, k \in \mathcal{Z}_{q'})$ denotes the messages to be passed from check node f_m^C to symbol node $\mathbf{C}_C(n)$. Suppose that $\{m_k\}, k \in \mathcal{Z}_{q'}$, denote the index-set of rows, which have the same target value (e.g. the elements at (11,11) in Tab. III) in one of q^2 PLNC mapping's check-relation-tab for PCD decoding. Therein, the element at (n, n) is generated as $\{k\}$ and

m_{tab} means the index of row.

For each PLNC mapping $\mathcal{M}_i, i \in \{0, 1, 2, 3\}$, we compute for each $[m, n]$ that satisfies $h_{mn} \neq 0$.

1. Initialization

Compute the initial value of each u_n^k based on

$$\begin{aligned} u_n^k &= \sum_{(\mathbf{C}_A(n), \mathbf{C}_B(n)): \mathbf{C}_C(n)=k} Pr((\mathbf{C}_A(n), \mathbf{C}_B(n)) | \mathbf{Y}_C(n)); \\ t_{nm} &= (u_n^k, k \in \mathcal{Z}_{q'}) = ((1/\beta_1)u_n^k, k \in \mathcal{Z}_{q'}); \\ \beta_1 &= \sum_{k \in \mathcal{Z}_{q'}} u_n^k. \end{aligned} \quad (16)$$

where $Pr((\mathbf{C}_A(n), \mathbf{C}_B(n)) | \mathbf{Y}_C(n))$ is the probability of $(\mathbf{C}_A(n), \mathbf{C}_B(n))$ given $\mathbf{Y}_C(n)$ is received.

2. First half round iteration

$$\begin{aligned} v_m^k &= \sum_{m_{tab} \in \{m_k\}} F_W(m_{tab}) \prod_{n' \in M_m \setminus n} t_{n'm}(m_{tab}); \\ w_{mn} &= (v_m^k, k \in \mathcal{Z}_{q'}), \end{aligned} \quad (17)$$

where $t_{n'm}(m_{tab})$ denotes that k of $(u_n^k, k \in \mathcal{Z}_{q'})$ is the designated elements at the m_{tab} -th row in the one of q^2 PLNC mapping's check-relation-tab for PCD decoding.

3. Second half round iteration

$$\begin{aligned} u_n^k &= p_k^{-(o_n-1)} u_n^k \prod_{m' \in N_n \setminus m} w_{m'n}; \\ t_{nm} &= (u_n^k, k \in \mathcal{Z}_{q'}) = ((1/\beta_2)u_n^k, k \in \mathcal{Z}_{q'}); \\ \beta_2 &= \sum_{k \in \mathcal{Z}_{q'}} u_n^k, \end{aligned} \quad (18)$$

where p_k denotes the average probability of occurrence of element k and o_n indicates column weight for the n -th symbol node. Let $P_n = \{p_k, k \in \mathcal{Z}_{q'}\}$, e.g., we have $P_n = \{\frac{1}{4}, \frac{1}{4}, \frac{1}{4}, \frac{1}{4}\}$ for \mathcal{M}_0 mapping and $P_n = \{\frac{1}{4}, \frac{1}{2}, \frac{1}{4}\}$ for \mathcal{M}_1 mapping, respectively.

4. Soft decision

$$\begin{aligned} U_n^k &= p_k^{-o_n} u_n^k \prod_{m \in N_n} w_{mn}; \\ T_{nm} &= (U_n^k, k \in \mathcal{Z}_{q'}) = ((1/\beta_3)U_n^k, k \in \mathcal{Z}_{q'}); \\ \beta_3 &= \sum_{k \in \mathcal{Z}_{q'}} U_n^k. \end{aligned} \quad (19)$$

5. Hard decision

$$\hat{\mathbf{C}}_C(n) = \arg \max_{\mathcal{M}_i \in \mathcal{Z}_{q'}} \sum_{k \in \mathcal{M}_i} U_n^k. \quad (20)$$

If C_C satisfies the applied \mathcal{M}_i mapping's check-relation-tab for virtual encoder or the number of iterations exceeds a certain value, then the algorithm stops, otherwise we go to Step 2. So far, the whole PCD algorithm for arbitrary PLNC mapping is presented.

C. Convergence behavior

There are many methods that can be used to investigate the convergence behavior of iterative decoding. Examples are the density evolution algorithm [34] and the extrinsic information transfer (EXIT) chart [35], both of which are suitable for LDPC codes over Gaussian channels. However, the virtual LDPC code, namely, check-relation-tab in the considered TWR model is different from conventional LDPC codes. Moreover, the proposed check-relation-tab is determined by the selected PLNC mapping. That is to say, several check-relation-tabs should be selected adaptively at the relay. To the best of our knowledge, there is no any literature to solve the analogous problem up to now. Similar to [21], we resort to simulations in Section VII for confirming the convergence behavior of the proposed PCD algorithm.

D. Complexity analysis

Note that the proposed PCD approach has only one constraint on the index of non-zero elements of two correlative rows. Therein, the two correlative rows belong to two different LDPC codes \mathbf{H}_A and \mathbf{H}_B at the two source nodes, respectively. It is because the proposed check-relation-tab should be generated under the constraint of the same index of non-zero elements of two correlative rows. Since the decoding complexity of the PCD approach is basically determined by the check-relation-tabs, we focus the complexity calculation on the number and size of the check-relation-tab. Let $M \times N$, d_r and r_κ denote the matrix size, the maximum row weight and the κ -th row weight in the well known degree distributions of an arbitrary irregular LDPC code, respectively. The number of the check-relation-tab for a given PLNC mapping, denoted as N_T , can be upper bounded

$$N_T \leq \sum_{r_\kappa=2}^{d_r} \min \left(\lambda_{r_\kappa} M, q^{2(r_\kappa-1)} \right) r_\kappa, \quad (21)$$

where λ_{r_κ} is the fraction of all rows with row weight r_κ . The equality can be reached when the non-zeros elements of any two rows are different each other. In theory, it is likely to generate different check-relation-tab when the row weight or the elements of this row are not the same as

each other. However, only one check-relation-tab for PCD decoder needs to be obtained for one or more selected adaptive PLNC mapping when the regular LDPC codes are applied and the non-zero elements in every row follows some special patters like $\{\eta, \dots, \eta\}, \eta \in \mathcal{Z}_q$. Otherwise, we also obtain the size of certain check-relation-tab for virtual encoder with a given PLNC mapping as

$$S_E = q'^{(r_\kappa - 1)}, \quad (22)$$

where q' denotes the range of PLNC mapped symbols at the relay, $q \leq q' \leq q^2$. Moreover, the size range of the check-relation-tab for PCD decoder is

$$q'^{(r_\kappa - 1)} \leq S_D \leq q^{r_\kappa}, \quad (23)$$

which is determined by the selected PLNC mapping and the applied optimizations. We will state it in Section VI concretely.

VI. APPLICATIONS OF PCD FOR TWO-WAY RELAY FADING CHANNELS

Recall that the design criterion of $\mathcal{M}(\mathbf{C}_A, \mathbf{C}_B)$ is to maximize the MED, as stated in Section IV. However, it is difficult to directly maximize the MED. In this section, we shall consider to optimize the symbol distance first and then the Hamming distance. Accordingly, we propose a new partial decoding realizations, two-stage CNC mapping with PCD (TS-CNC-PCD), for TWR fading channels. The same (3,6) Tanner graph shown in Fig. 3(a) is used for illustration purpose.

A. Two-stage CNC mapping with PCD (TS-CNC-PCD)

In this method, the CNC mapping proposed in [22] is divided to two steps for maximizing the symbol distance first and then the MCO based on the proposed PCD approach is presented to optimize the Hamming distance.

1) *Channel coding structure at the relay:* The proposed TS-CNC-PCD is composed of the first CNC mapper ($\mathbf{GF}(q + p_2)$), PCD decoder ($\mathbf{GF}(q + p_2)$), the second CNC mapper ($\mathbf{GF}(q + p_1)$) and $(q + p_1)$ PSK/QAM modulator as shown in Fig. 4(a). Upon receiving the superimposed packet, the relay initializes the soft value for PCD decoder by taking into account the 1st CNC mapping. The output of the PCD decoder, i.e., the 2nd CNC mapped codeword packet, $\mathbf{C}_C = \mathcal{M}(\mathbf{C}_A, \mathbf{C}_B)$, is then modulated to $(q + p_1)$ PSK/QAM accordingly to obtain \mathbf{X}_C . Note that $\{p_1, p_2\} \in \mathcal{Z}_{q^2 - q}$ represents the possible expanding of cardinality (e.g., $p_1 = 0(1), p_2 = 5(8)$ for the QPSK(5QAM) when QPSK ($q = 4$) is used at two sources). \mathcal{M} denotes a kind of CNC mapping.

2) *Two-stage CNC mapping*: Since Koike-Akino *et al* have presented the best CNC mappings for the QPSK modulation in the Table I in [22], we just use for reference and generate the two-stage CNC mapping. In terms of maximizing the symbol distance between two CNC mapped symbols in a codeword, we divide the traditional CNC mapping into the 1st CNC mapping (named as $\mathcal{M}_i^s, i \in [0, 11]$) and the 2nd CNC mapping (named as $\mathcal{M}_j^h, j \in [0, 5]$) for soft value initialization and hard value decision, respectively. Take Fig. 2(a) for example, we only group together some symbol pairs (e.g. (0,1) and (1,0) in \mathcal{M}_0^s), which are more closer each other, while classify the other symbol pairs (e.g. (2,3) and (3,2)), which are more far away from (0,1) or (1,0), into another independent cluster. Certainly, these separated clusters (e.g. (0,1),(1,0),(2,3) and (3,2)) are mapped to one cluster again in \mathcal{M}_0^h . Similarly, $\mathcal{M}_1^s/\mathcal{M}_1^h$ and $\mathcal{M}_4^s/\mathcal{M}_2^h$ are generated according to Fig. 2(b) and (c). Tab. IV shows all maps given by the two-stage CNC mapping when QPSK is applied at two sources. Here, to avoid confusion, we let $\{a', b', c', \dots\}$ indicate the broadcasted symbols $\{0, 1, 2, \dots\}$, which are not same as the decoding symbols $\{a, b, c, \dots\}$ during the period of operating PCD algorithm.

3) *Check-relation-tab*: Note that only the 1st CNC mapping ($\mathcal{M}_i^s, i \in [0, 11]$) are operated before soft iteration in the proposed PCD approach, we just need to generate the check-relation-tabs according to ($\mathcal{M}_i^s, i \in [0, 11]$). Take the \mathcal{M}_4^s mapping of Tab. IV for example, which is displayed in Fig. 2(c). Each symbol pair $(C_A(n), C_B(n))$ is mapped to one of the twelve elements based on the fading conditions $H_{BC}/H_{AC} \simeq (1+j)/2$. All the possible mappings are listed below: $\{a\}:(0, 1), (1, 2)$; $\{b\}:(0, 3), (2, 0)$; $\{c\}:(1, 3), (3, 0)$; $\{d\}:(2, 1), (3, 2)$; $\{e\}:(0, 0)$; $\{f\}:(0, 2)$; $\{g\}:(1, 0)$; $\{h\}:(1, 1)$; $\{i\}:(2, 2)$; $\{j\}:(2, 3)$; $\{k\}:(3, 1)$; $\{l\}:(3, 3)$. Each element constrained by the check functions f_n^C corresponds to one symbol pair in $\{(C_A(n), C_B(n)), n \in \{0, 2, 4, 6, 8, 11\}\}$, the range of which is in $\{a, b, c, d, e, f, g, h, i, j, k, l\}$. Similar to the Section V, we can obtain the check-relation-tabs for all 1st CNC mappings ($\mathcal{M}_i^s, i \in [0, 11]$) easily.

B. Minimum correlation optimization (MCO)

Due to the irregular cardinality of the 1st CNC mappings $\mathcal{M}_i^s(i \in [0, 11])$, the sizes of mostly generated check-relation-tabs for PCD decoder can approach the maximum value, i.e. $S_D = q^{r\kappa}$. That is to say, we can not obtain larger coding gains from these check-relation-tabs. Note that the check-relation-tabs are fixed once a PLNC mapping and the correlative rows of two LDPC codes (\mathbf{H}_A and \mathbf{H}_B) are all selected. Therefore, a kind of correlative rows optimization, named as the

minimum correlation optimization (MCO), is proposed for selecting the better check-relation-tab.

Using the proposed MCO method (Algorithm 1), we obtain a collection of non-zero elements distribution for the correlative rows of \mathbf{H}_A and \mathbf{H}_B . Considering the trade-off of complexity and performance, we select a special correlative rows like $\{\eta, \dots, \eta\}, \eta \in \mathcal{Z}_q$. For instance, the check-relation-tabs for some mappings ($\mathcal{M}_i^s, i \in \{0, 1, 4\}$) can be generated as shown in V.

C. Simplification of TS-CNC-PCD

For simplicity, the two-stage CNC mapping can be integrated into one-stage mapping. That is to say, the identical mapping is used for soft value initialization and hard value decision. As shown in Fig. 4(b), the simplification of TS-CNC-PCD is composed of an adaptive CNC mapper ($\text{GF}(q + p_1)$), PCD decoder ($\text{GF}(q + p_1)$) and $(q + p_1)$ PSK/QAM modulator. According to the same design principle, we can generate the corresponding check-relation-tabs. The expected error performance may be worse. However, the complexity (size of check-relation-tab) is decreased dramatically. More details can be found in [1], [2].

VII. SIMULATION RESULTS

In this section, we present some simulation results to illustrate the convergence behaviors and the coding gains of the proposed PCD approach. For simplicity, each node uses the same transmission power 1 and observes the same noise power σ^2 . Define an average SNR per information symbol as $\frac{1}{2R\sigma^2}$, where R is the channel code rate. According to the proposed MCO method, we generate a 4-ary code from a binary LDPC code "252.252.3.252", which is produced by Mackay [36], through replacing $\{1, \dots, 1\}$ by $\{\eta, \dots, \eta\}, \eta \in \mathcal{Z}_4$. Code length, code rate, row weight and column weight are 504, 0.5, 6 and 3, respectively.

The proposed partial decoding method, TS-CNC-PCD, is simulated in kinds of TWR channels. The selections for the two-stage CNC mapping and traditional CNC mapping are based on instantaneous realizations of the channel gain pairs (CGP) $\{\mathbf{H}_{AC}, \mathbf{H}_{BC}\}$ using Fig. 5 (a,b) and Fig. 5 (b), respectively.

For comparison, two benchmark systems are considered. One is the uncoded case, where QPSK modulation is applied and the relay demodulates using kinds of PLNC mappings. The other is the coded conventional XOR case, where the same 4-ary LDPC is applied at the source and the relay performs traditional BP decoding with conventional XOR mapping.

A. TWR Gaussian channels

Fig. 6 shows the convergence behaviors of the proposed PCD algorithm with three kinds of channel gain pairs and Gaussian noise. Three maximum iterations are selected as 10, 20 and 30. In general, larger maximum iteration leads to better performance for the proposed TS-CNC-PCD method no matter any channel gain pair is considered, as shown in Fig. 6(a,b,c). Obviously, the proposed PCD algorithm has wonderful convergence behaviors.

We can see that the same observations for uncoded XOR and CNC are shown in Fig. 6(a). It is because the CNC mapping is degraded to XOR mapping when the channel gain pair is set as $H_{AC} = H_{BC} = 1$. Interestingly, the proposed TS-CNC-PCD is a little bit better than the XOR-BP. It is clear that the coding gains of all considered coded systems are more than 3.5dB compared to the uncoded scenarios at $\text{SER} = 10^{-3}$. From Fig. 6(b), we can see that the XOR mapping and XOR-BP coding method do not work well. Fortunately, the coding gains of TS-CNC-PCD is also more than 3.5dB compared to the uncoded CNC at $\text{SER} = 10^{-3}$. Lastly, as shown in Fig. 6(c), the XOR-BP coding method outperforms the uncoded CNC more than 1.25dB at $\text{SER} = 10^{-3}$ while the uncoded XOR mapping still does not work well. At the same time, the proposed TS-CNC-PCD obtains more than 2dB coding gain compared to the XOR-BP at $\text{SER} = 10^{-3}$. In general, our proposed TS-CNC-PCD not only obtains the best performance but also achieves the constant coding gain in considered TWR Gaussian channels.

B. TWR block fading channels

Suppose that the channel gains on all links follow Rayleigh or Rice distribution and are independent. We assume $E[|H_{AC}|^2] = E[|H_{BC}|^2] = 1$, where notation $E[\cdot]$ denotes expectation function. The black solid lines, denoted as "Outage Probability", are actually the lower bound of the outage probability of the TWR block fading channels according to (8). The maximum iteration is fixed at 30 for the coded cases.

Fig. 7(a) shows the FER performance of the Rayleigh channels. For the uncoded cases, the CNC outperforms the XOR about 4 dB at $\text{FER} = 1.8 \times 10^{-3}$. At the same FER, the coding gain of the coded XOR is about 8.5 dB. Moreover, the coding gain of the coded CNC is about 6 dB at $\text{FER} = 7.5 \times 10^{-4}$. Why the coding gain of TS-CNC-PCD is less than that of XOR-BP? It is because the uncoded denoising mapping used at the relay node can eliminate part of the noise, as confirmed in [22]. We also see that the TS-CNC-PCD outperforms the XOR-BP about 2 dB

at $\text{FER} = 2.8 \times 10^{-4}$. At the same time, the gap between the coded XOR and the lower bound of the outage probability is about 6.5 dB while the gap for the TS-CNC-PCD is 4.5 dB. By any possibility, we can reduce the gaps when the code length and the maximum iteration approach infinity.

The similar observations can be seen in Fig. 7(b) where the channel becomes Rice fading with the Rician factor 0 dB. For the uncoded cases, the XOR is worse than the CNC about 4.5 dB. At $\text{FER} = 4.8 \times 10^{-3}$, the coding gain of the coded XOR is 9.2 dB. We also observe that TS-CNC-PCD has about 6.7 dB at $\text{FER} = 1.8 \times 10^{-3}$ in terms of coding gain. It is clear that the TS-CNC-PCD is better than the coded XOR about 1.7 dB at $\text{FER} = 5.8 \times 10^{-4}$. Simultaneously, the coded XOR has a gap of 6.2 dB from the outage probability while the TS-CNC-PCD has about 4.5 dB. Intuitively, the longer code length and the larger maximum iteration lead to the smaller gap.

Lastly, it is important to see that both the relay and the sources have the same FER performance no matter which one of the TWR fading channels is considered. These phenomena confirm that the errors at the relay have severe impact on the performance of whole system. It is also shown that the proposed PCD algorithm is necessary and effective.

VIII. CONCLUSION

In this paper, maintaining the traditional channel coding structure at the two sources, we propose a new channel coding solution at the relay, called *pairwise check decoding*, or *PCD*, for applying the adaptive PLNC mapping. The check-relation-tab for the superimposed LDPC-coded packet pair at relay is formed according to the selected PLNC mapping. Emphatically, the proposed PCD algorithm is universal for any adaptive PLNC mapping under the constraint of exclusive law. In order to optimize the MED, we also present a partial decoding method at the relay, TS-CNC-PCD, for LDPC coded TWR block fading channels. Moreover, a check-relation-tab optimization MCO is introduced to improve performance. Simulation results confirm that the proposed TS-CNC-PCD has wonderful convergence behaviors along with the maximum iteration increasing and significant coding gains compared to the uncoded system for certain TWR Gaussian channels. For TWR fading channels, the TS-CNC-PCD also outperforms the conventional XOR with BP obviously.

REFERENCES

- [1] J. Liu, M. Tao, Y. Xu, and X. Wang, "Pairwise check decoding for LDPC coded two-way relay fading channels," in *Proc. IEEE Int. Conf. Comm. (ICC)*, May 2010.
- [2] J. Liu, M. Tao, and Y. Xu, "Pseudo exclusive-or for LDPC coded two-way relay block fading channels," in *Proc. IEEE Int. Conf. Comm. (ICC)*, June 2011.
- [3] Y. Wu, P. A. Chou, and S.-Y. Kung, "Information exchange in wireless networks with network coding and physical-layer broadcast," in *Proc. Conf. Inform. Sciences Systems (CISS)*, Mar. 2005.
- [4] P. Larsson, N. Johansson, and K.-E. Sunell, "Coded bi-directional relaying," in *Proc. Scandinavian Workshop Ad Hoc Networks (ADHOC)*, May 2005.
- [5] P. Popovski and H. Yomo, "Bi-directional amplification of throughput in a wireless multi-hop network," in *Proc. IEEE Veh. Tech. Conf. (VTC)*, May 2006, pp. 588–593.
- [6] C. Hausl and J. Hagenauer, "Iterative network and channel decoding for the two-way relay channel," in *Proc. IEEE Int. Conf. Comm. (ICC)*, Jun. 2006, pp. 1568–1573.
- [7] S. Zhang, S. C. Liew, and P. P. Lam, "Physical-layer network coding," in *Proc. ACM Annual Int. Conf. Mobile Computing Networking (MobiCom)*, Sept. 2006, pp. 358–365.
- [8] S. Katti, H. Rahul, W. Hu, D. Katabi, M. M. edard, and J. Crowcroft, "XORs in the air: Practical wireless network coding," in *Proc. ACM SIGCOMM*, Sept. 2006, pp. 243–254.
- [9] B. Rankov and A. Wittneben, "Spectral efficient protocols for half-duplex fading relay channels," *IEEE Jour. Sel. Areas. Comm.*, vol. 25, no. 2, pp. 379–389, Feb. 2007.
- [10] R. Ahlswede, N. Cai, S.-Y. R. Li, and R. W. Yeung, "Network information flow," *IEEE Trans. Inform. Theory*, vol. 46, no. 4, pp. 1204–1216, July 2000.
- [11] T. J. Oechtering, C. Schnurr, I. Bjelakovic, and H. Boche, "Broadcast capacity region of two-phase bidirectional relaying," *IEEE Trans. Inform. Theory*, vol. 54, no. 1, pp. 454–458, Jan. 2008.
- [12] S. J. Kim, P. Mitran, and V. Tarokh, "Performance bounds for bi-directional coded cooperation protocols," *IEEE Trans. Inform. Theory*, vol. 54, no. 11, pp. 5235–5241, Nov. 2008.
- [13] C. Schnurr, S. Stanczak, and T. J. Oechtering, "Achievable rates for the restricted half-duplex two-way relay channel under a partial-decode-and-forward protocol," in *Proc. IEEE Inform. Theory Workshop (ITW)*, May 2008, pp. 134–138.
- [14] D. Gunduz, E. Tuncel, and J. Nayak, "Rate regions for the separated two-way relay channel," in *Proc. Annual Allerton Conf. Comm. Control Computing*, Sept. 2008, pp. 1333–1340.
- [15] S. J. Kim, N. Devroye, P. Mitran, and V. Tarokh, "Achievable rate regions for bi-directional relaying," May 2009. [Online]. Available: <http://arxiv.org/abs/0808.0954>
- [16] P. Popovski and H. Yomo, "Physical network coding in two-way wireless relay channels," in *Proc. IEEE Int. Conf. Comm. (ICC)*, June 2007, pp. 707–712.
- [17] W. Nam, S.-Y. Chung, and Y. H. Lee, "Capacity bounds for two-way relay channel," in *Proc. Int. Zurich Seminar Comm. (IZS)*, March 2008, pp. 144–147.
- [18] B. Nazer and M. Gastpar, "The case for structured random codes in network communication theorems," in *Proc. Inform. Theory Workshop (ITW)*, Sept. 2007.
- [19] K. Narayanan, M. P. Wilson, and A. Sprintson, "Joint physical layer coding and network coding for bi-directional relaying," in *Proc. Allerton Conf. Comm., Control and Computing*, 2007.

- [20] M. P. Wilson, K. Narayanan, H. Pfister, and A. Sprintson, "Joint physical layer coding and network coding for bi-directional relaying," May 2008. [Online]. Available: <http://arxiv.org/abs/0805.0012v2>
- [21] S. Zhang and S.-C. Liew, "Channel coding and decoding in a relay system operated with physical-layer network coding," *IEEE Jour. Sel. Areas. Comm.*, vol. 27, no. 5, pp. 788–796, June 2009.
- [22] T. Koike-Akino, P. Popovski, and V. Tarokh, "Optimized constellations for two-way wireless relaying with physical network coding," *IEEE Jour. Sel. Areas. Comm.*, vol. 27, no. 5, pp. 773–787, June 2009.
- [23] —, "Denoising strategy for convolutionally-coded bidirectional relaying," in *Proc. IEEE Int. Conf. Comm. (ICC)*, 2009.
- [24] A. Burr, *Modulation and Coding for Wireless Communications*. Addison-Wesley Longman Publishing Co., Inc., 2001.
- [25] D. Declercq and M. Fossorier, "Decoding algorithms for nonbinary LDPC codes over GF(q)," *IEEE Trans. Comm.*, vol. 55, no. 4, pp. 633–643, April 2007.
- [26] C. Poulliat, M. Fossorier, and D. Declercq, "Design of regular (2, dc)-LDPC codes over GF(q) using their binary images," *IEEE Trans. Comm.*, vol. 56, no. 10, pp. 1626–1635, October 2008.
- [27] G. Li, I. J. Fair, and W. A. Krzymien, "Density evolution for nonbinary LDPC codes under Gaussian approximation," *IEEE Trans. Inform. Theory*, vol. 55, no. 3, pp. 997–1015, March 2009.
- [28] E. Biglieri, J. Proakis, and S. Shamai, "Fading channels: information-theoretic and communications aspects," *IEEE Trans. Inform. Theory*, vol. 44, no. 6, pp. 2619–2692, October 1998.
- [29] G. Ungerboeck, "Channel coding with multilevel/phase signals," *IEEE Trans. Inform. Theory*, vol. IT-28, no. 1, pp. 55–67, January 1982.
- [30] J. M. Wozencraft and I. M. Jacobs, *Principles of communication engineering*. John Wiley & Sons Inc., 1965.
- [31] R. Knopp and P. A. Humblet, "On coding for block fading channels," *IEEE Trans. Inform. Theory*, vol. 46, no. 1, pp. 189–205, January 2000.
- [32] R. Gallager, "Low-density parity-check codes," *IRE Trans. Inform. Theory*, pp. 21–28, Jan. 1962.
- [33] T. J. Richardson, M. A. Shokrollahi, and R. L. Urbanke, "Design of capacity-approaching irregular low-density parity-check codes," *IEEE Trans. Inform. Theory*, vol. 47, no. 2, pp. 619–637, February 2001.
- [34] T. J. Richardson and R. L. Urbanke, "The capacity of low-density parity-check codes under message-passing decoding," *IEEE Trans. Inform. Theory*, vol. 47, no. 2, pp. 599–618, February 2001.
- [35] S. ten Brink, "Convergence behavior of iteratively decoded parallel concatenated codes," *IEEE Trans. Comm.*, vol. 49, no. 10, pp. 1727–1737, October 2001.
- [36] D. J. C. Mackay, "Encyclopedia of sparse graph codes," Sep. 2009. [Online]. Available: <http://www.inference.phy.cam.ac.uk/mackay/codes>

Data: given $r_\kappa, q, q', \mathcal{M}$

Result: a collection of non-zero elements distribution for the correlative rows

```

1 Initialization:  $\{\eta_1, \eta_2, \dots, \eta_{r_\kappa}\} = \{1, 1, \dots, 1\}, \{\xi_1, \xi_2, \dots, \xi_{r_\kappa}\} = \{1, 1, \dots, 1\}$  ;
2 Set the expected collection:  $C_{exp} = \emptyset$ ;
3 Set the maximum average number of possible generation:  $G_{max} = q'$ ;
4 while  $\eta_1 < q$  do
5    $\forall \mathcal{M}_i \in \mathcal{M}$ , generate the relevant check-relation tabs;
6   Let the temporary value  $G_{max_{temp}}$  equal to the maximum average number of possible
   generations of the lastly check-relation tabs;
7   if  $G_{max_{temp}} \leq G_{max}$  then
8     if  $G_{max_{temp}} = G_{max}$  then
9       | Add  $\{\eta_1, \eta_2, \dots, \eta_{r_\kappa}\}, \{\xi_1, \xi_2, \dots, \xi_{r_\kappa}\} \rightarrow C_{exp}$  ;
10      else
11        | Set  $G_{max} = G_{max_{temp}}, C_{exp} = \emptyset$ , add  $\{\eta_1, \eta_2, \dots, \eta_{r_\kappa}\}, \{\xi_1, \xi_2, \dots, \xi_{r_\kappa}\} \rightarrow C_{exp}$ ;
12      end
13    end
14    if  $\xi_n(\eta_n) = q, n \in [2, r_\kappa]$  then
15      |  $\xi_n(\eta_n) = 1, \xi_{n-1}(\eta_{n-1}) = \xi_{n-1}(\eta_{n-1}) + 1$ ;
16    else
17      |  $\xi_{r_\kappa} = \xi_{r_\kappa} + 1$ ;
18    end
19    if  $\xi_1 = q$  then
20      |  $\{\xi_1, \xi_2, \dots, \xi_{r_\kappa}\} = \{1, 1, \dots, 1\}, \eta_{r_\kappa} = \eta_{r_\kappa} + 1$ ;
21    end
22 end

```

Algorithm 1: Minimum correlation optimization (MCO)

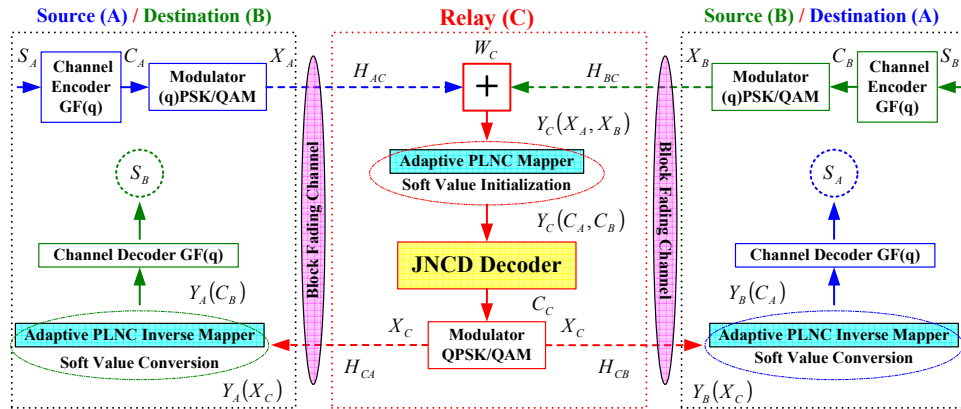


Fig. 1: Channel coding model for TWR block fading channels.

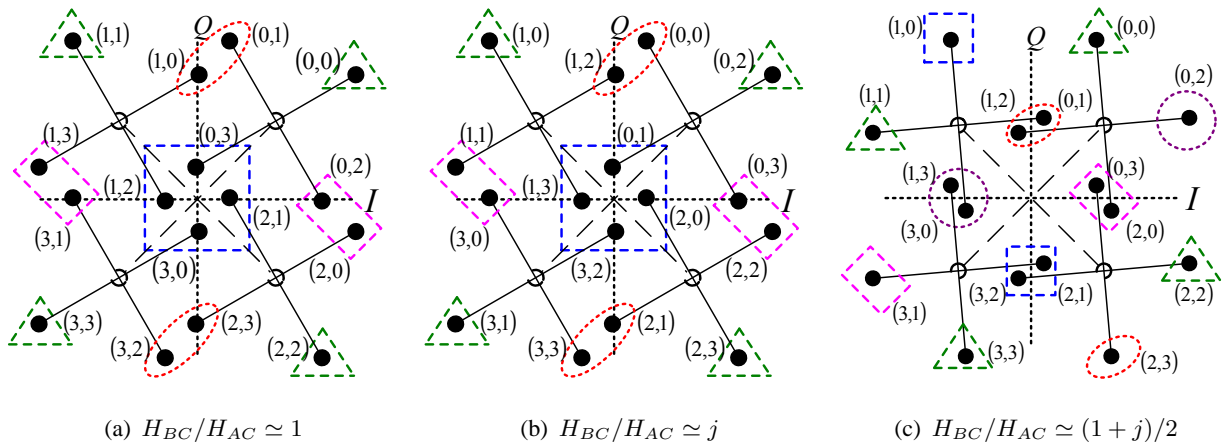
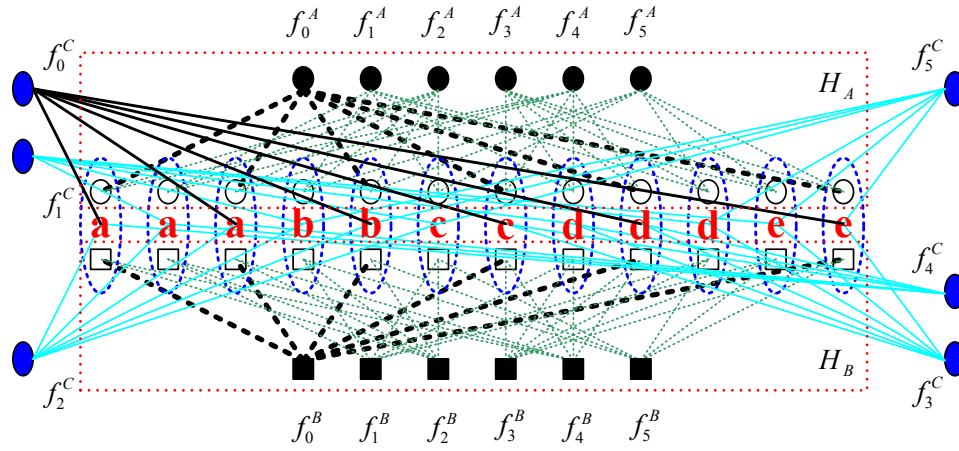


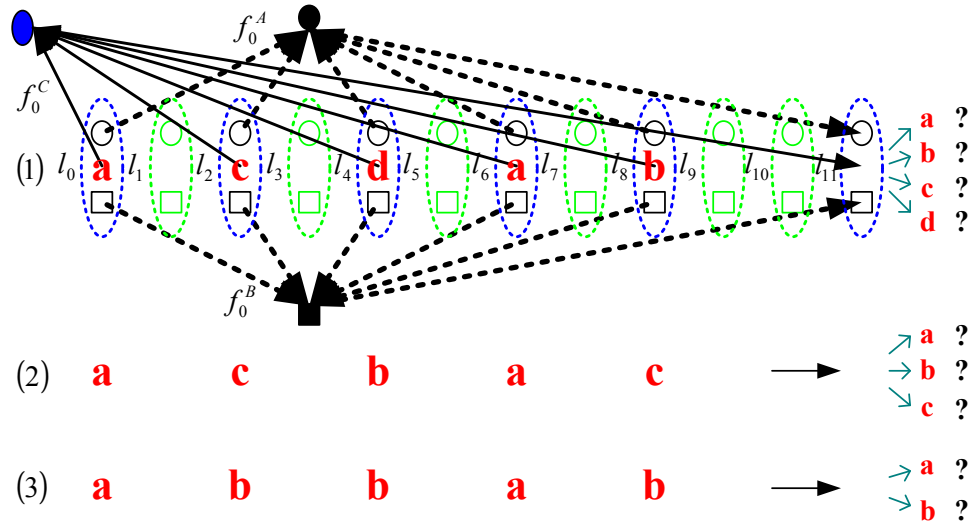
Fig. 2: Received signal constellation with CNC mapping at the relay.

TABLE I: 4 possible PLNC mappings for the binary LDPC codes

	\mathcal{M}_0	\mathcal{M}_1	\mathcal{M}_2	\mathcal{M}_3
(0, 0)	a	a	a	a
(0, 1)	b	b	b	b
(1, 0)	c	b	c	b
(1, 1)	d	c	a	a
Cardinality	4	3	3	2



(a) Panoramic Tanner graph



(b) Segmental Tanner graph

Fig. 3: The Tanner graph of the check functions versus symbol pairs at the relay.

TABLE II: Check-relation-tab of f_0^C for virtual encoder with binary LDPC codes

	(0, 0)	(2, 2)	(4, 4)	(6, 6)	(8, 8)	(11, 11)
\mathcal{M}_0 1024×6	a	a	a	a	a	a
	a	a	a	a	b	b
	a	a	a	a	c	c
	\vdots	\vdots	\vdots	\vdots	\vdots	\vdots
	d	d	d	d	c	c
	d	d	d	d	d	d
\mathcal{M}_1 243×6	a	a	a	a	a	a
	a	a	a	a	b	b
	a	a	a	a	c	c
	\vdots	\vdots	\vdots	\vdots	\vdots	\vdots
	c	c	c	c	b	b
	c	c	c	c	c	c
\mathcal{M}_2 243×6	a	a	a	a	a	a
	a	a	a	a	b	b, c
	a	a	a	a	c	b, c
	\vdots	\vdots	\vdots	\vdots	\vdots	\vdots
	c	c	c	c	b	b
	c	c	c	c	c	c
\mathcal{M}_3 32×6	a	a	a	a	a	a
	a	a	a	a	b	b
	a	a	a	b	a	b
	\vdots	\vdots	\vdots	\vdots	\vdots	\vdots
	b	b	b	b	a	a
	b	b	b	b	b	b

TABLE III: Check-relation-tab of f_0^C for PCD decoder with binary LDPC codes

	(11, 11)	F_W	(0, 0)	(2, 2)	(4, 4)	(6, 6)	(8, 8)
\mathcal{M}_0 1024×7	a	1	a	a	a	a	a
	a	1	a	a	a	b	b
	a	1	a	a	a	c	c
	\vdots	\vdots	\vdots	\vdots	\vdots	\vdots	\vdots
	d	1	d	d	d	c	c
	d	1	d	d	d	d	d
\mathcal{M}_1 333×7	a	1	a	a	a	a	a
	a	0.5	a	a	a	b	b
	a	1	a	a	a	c	c
	\vdots	\vdots	\vdots	\vdots	\vdots	\vdots	\vdots
	c	0.5	c	c	c	b	b
	c	1	c	c	c	c	c
\mathcal{M}_2 333×7	a	1	a	a	a	a	a
	a	1	a	a	a	b	b
	a	1	a	a	a	b	c
	\vdots	\vdots	\vdots	\vdots	\vdots	\vdots	\vdots
	c	1	c	c	c	b	b
	c	1	c	c	c	c	c
\mathcal{M}_3 32×7	a	1	a	a	a	a	a
	a	1	a	a	a	b	b
	a	1	a	a	b	a	b
	\vdots	\vdots	\vdots	\vdots	\vdots	\vdots	\vdots
	b	1	b	b	b	a	a
	b	1	b	b	b	b	b

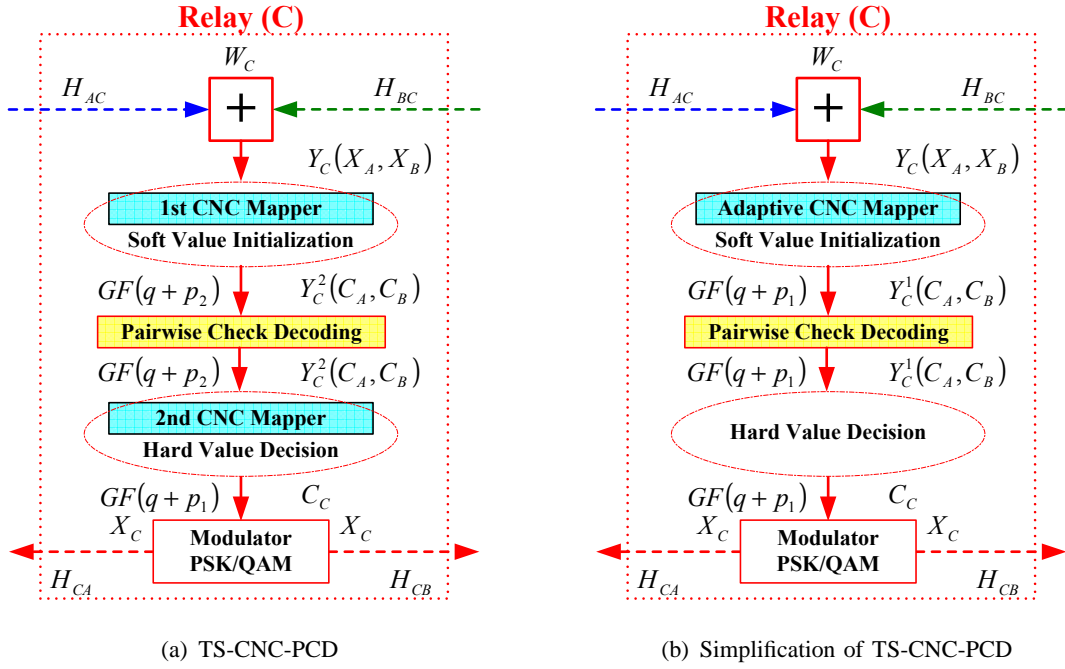


Fig. 4: Partial decoding model at the relay node for TWR fading channels.

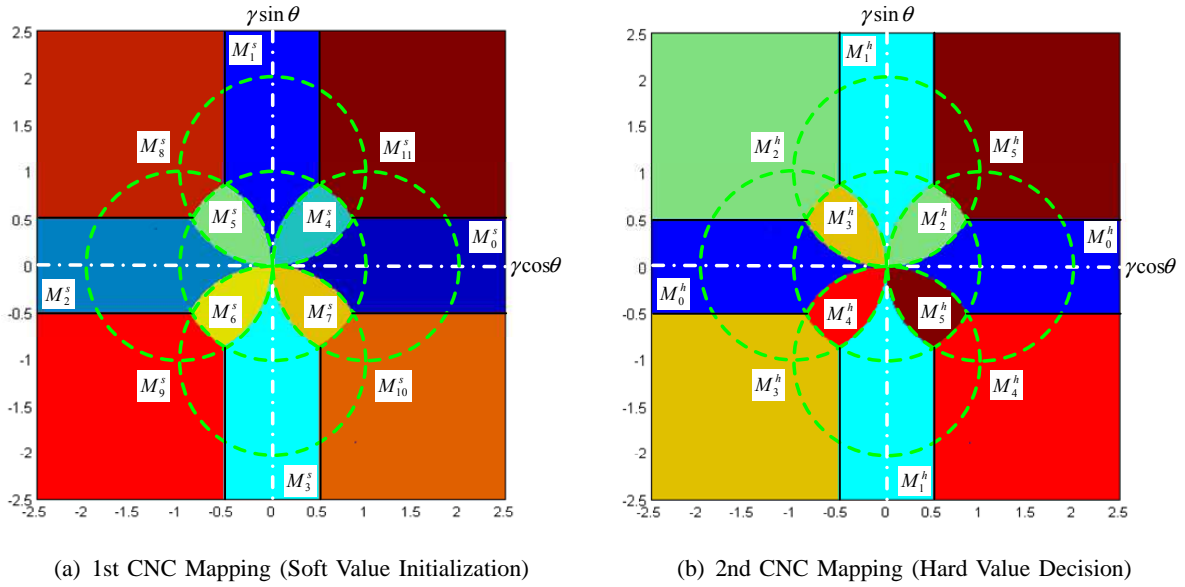


Fig. 5: Two-stage CNC mapping according to the channel ratio $\mathbf{H}_{BC}/\mathbf{H}_{AC} = \gamma(\cos \theta + j \sin \theta)$ when $q = 2^2$.

TABLE IV: Two-stage CNC mappings for 4-ary LDPC codes

	(0, 0)	(0, 1)	(0, 2)	(0, 3)	(1, 0)	(1, 1)	(1, 2)	(1, 3)	(2, 0)	(2, 1)	(2, 2)	(2, 3)	(3, 0)	(3, 1)	(3, 2)	(3, 3)	Cardinality
\mathcal{M}_0^s	f	b	c	a	b	g	a	d	c	a	h	e	a	d	e	i	9
\mathcal{M}_2^s	a	b	c	f	d	a	g	c	e	h	a	b	i	e	d	a	9
\mathcal{M}_0^h	a'	b'	c'	d'	b'	a'	d'	c'	c'	d'	a'	b'	d'	c'	b'	a'	4
\mathcal{M}_1^s	b	a	f	c	g	d	b	a	a	e	c	h	d	i	a	e	9
\mathcal{M}_3^s	b	f	a	c	a	c	d	g	h	b	e	a	e	a	i	d	9
\mathcal{M}_1^h	a'	b'	c'	d'	c'	d'	a'	b'	b'	a'	d'	c'	d'	c'	b'	a'	4
\mathcal{M}_4^s	e	a	f	b	g	h	a	c	b	d	i	j	c	k	d	l	12
\mathcal{M}_8^s	e	f	a	b	c	g	d	h	i	c	j	d	a	b	k	l	12
\mathcal{M}_2^h	b'	c'	a'	d'	a'	d'	c'	e'	d'	b'	e'	a'	e'	a'	b'	c'	5
\mathcal{M}_5^s	a	b	e	f	g	c	h	a	d	i	b	j	k	l	c	d	12
\mathcal{M}_9^s	a	e	b	f	c	d	g	h	i	j	c	d	k	a	l	b	12
\mathcal{M}_3^h	b'	c'	d'	a'	c'	e'	a'	b'	d'	a'	c'	e'	a'	b'	e'	d'	5
\mathcal{M}_6^s	a	e	b	f	c	b	g	h	i	j	d	a	k	d	l	c	12
\mathcal{M}_{10}^s	a	b	e	f	g	c	h	d	c	i	d	j	k	l	a	b	12
\mathcal{M}_4^h	b'	a'	c'	d'	e'	c'	b'	a'	a'	e'	d'	b'	c'	d'	a'	e'	5
\mathcal{M}_7^s	e	f	a	b	b	g	c	h	i	a	j	d	d	c	k	l	12
\mathcal{M}_{11}^s	e	a	f	b	g	h	c	d	c	d	i	j	a	k	b	l	12
\mathcal{M}_5^h	a'	b'	c'	d'	d'	a'	e'	c'	e'	c'	a'	b'	b'	e'	d'	a'	5

TABLE V: Check-relation-tabs of f_0^C for PCD decoder optimized by MCO

	(11, 11)	F_W	(0, 0)	(2, 2)	(4, 4)	(6, 6)	(8, 8)
$\mathcal{M}_0^s(\mathcal{M}_1^s)$ 110889 \times 7	a	1	a	a	a	a	a
	a	1	a	a	a	b	b
	a	1	a	a	a	b	e
	\vdots	\vdots	\vdots	\vdots	\vdots	\vdots	\vdots
	i	1	i	i	i	h	h
	i	1	i	i	i	i	i
\mathcal{M}_4^s 511872 \times 7	a	1	a	a	a	a	a
	a	0.5	a	a	a	b	b
	a	0.5	a	a	a	b	g
	\vdots	\vdots	\vdots	\vdots	\vdots	\vdots	\vdots
	l	1	l	l	l	k	k
	l	1	l	l	l	l	l

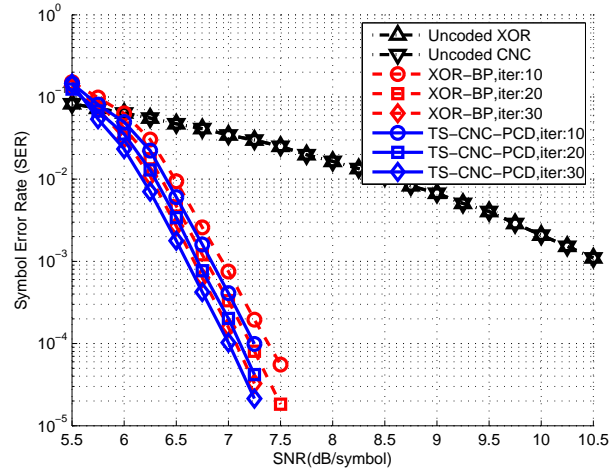
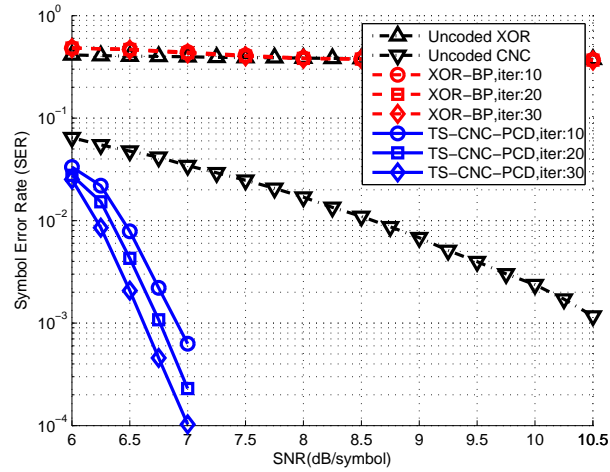
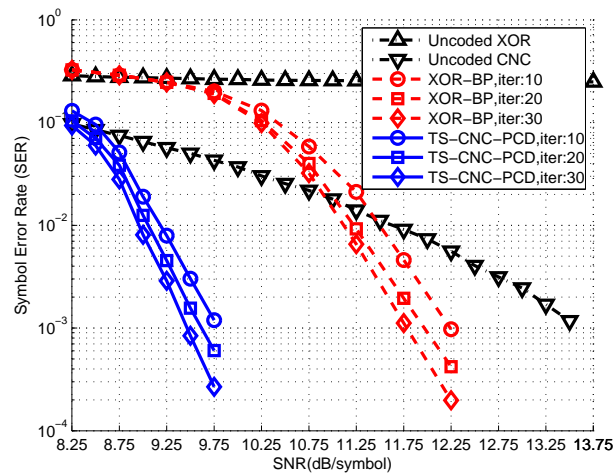
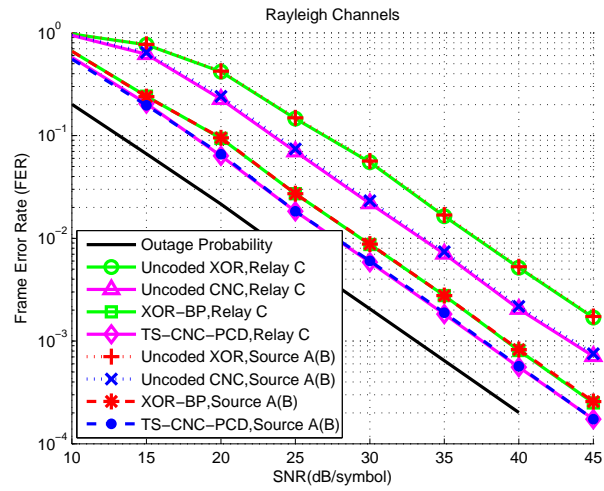
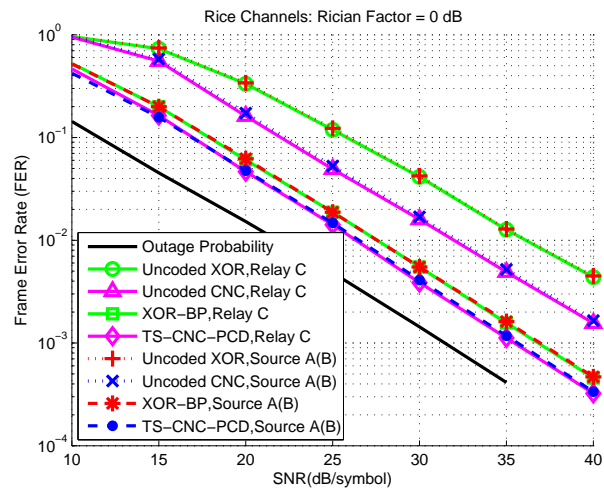
(a) $H_{AC} = H_{BC} = 1$ (b) $H_{AC} = 1, H_{BC} = j$ (c) $H_{AC} = 1, H_{BC} = (1 + j)/2$

Fig. 6: Convergence behaviors of the proposed PCD algorithm.



(a) Rayleigh channels



(b) Rice channels

Fig. 7: Performance comparisons in the TWR block fading channels.